# Tuneable Singlet Exciton Fission and Triplet–Triplet Annihilation in an Orthogonal Pentacene Dimer

*Steven Lukman, Andrew J. Musser, Kai Chen, Stavros Athanasopoulos, Chaw K. Yong, Zebing Zeng, Qun Ye, Chunyan Chi, Justin M. Hodgkiss, Jishan Wu,* Richard H. Friend, and Neil C. Greenham**

**Fast and highly efficient intramolecular singlet exciton fission in a pentacene dimer, consisting of two covalently attached, nearly orthogonal pentacene units is reported. Fission to triplet excitons from this ground state geometry occurs within 1 ps in isolated molecules in solution and dispersed solid matrices. The process exhibits a sensitivity to environmental polarity and competes with geometric relaxation in the singlet state, while subsequent triplet decay is strongly dependent on conformational freedom. The near orthogonal arrangement of the pentacene units is unlike any structure currently proposed for efficient singlet exciton fission and may lead to new molecular design rules.**

## 1. Introduction

The maximum efficiency of solar cells is limited by the thermalization of high-energy excitons generated through the absorption of photons well above the band gap.[1] One way to circumvent this limitation is to convert these high-energy states into multiple lower-energy excitons. In organic materials, this process is accomplished by singlet exciton fission (SEF), which consists of the separation of a singlet exciton into two low-energy triplet excitons, located on separate chromophores but initially coupled into an overall spin-zero configuration.[2] Thanks to this coupling, SEF is a spin-allowed process and can proceed on ultrafast (≈100 fs) time scales, allowing it to out-compete other decay channels and achieve high efficiencies.[3] The essential condition for efficient SEF is the energetic alignment of the singlet and triplet states, such that $2E(T_1) \leq E(S_1)$. A recent combined theoretical and experimental study of SEF rates in a range of acene solids has demonstrated that the rate of SEF is also greatly affected by the strength of intermolecular coupling within the film.[4] In the canonical system, pentacene, triplet pair formation is exothermic and the intermolecular coupling is strong, resulting in SEF with an 80 fs time constant and nearly 200% yield.[5]

Though most experimental studies of SEF have involved crystalline, polycrystalline or amorphous solids, the most basic unit capable of SEF is a pair of chromophores. Indeed, it was recently demonstrated in concentrated solutions of TIPS-pentacene that singlet fission can proceed at high efficiency through bimolecular diffusional interactions.[6] However, early attempts to directly control the interaction between chromophores through the use of covalent dimers have not been as successful. The most notable systems in this regard are tetracene and 1,3-diphenylisobenzofuran. These materials are found to exhibit efficient SEF in the solid state, but their covalent dimers achieved triplet yields of only a few percent. In both of these studies,[7] the two SEF chromophores were joined by a range of linkers to modify the strength of the electronic coupling between them, with the aim of tuning the rate and efficiency of SEF. The impact was subtle, and it thus remains unclear why covalent dimers have proved inefficient to date. Current models suggest that dimers should be asymmetric or contain significant cofacial interaction between chromophores to attain high triplet yields.[2,8] Interestingly, a recent study of pentacene dimers separated by a phenyl spacer unit achieved triplet yields above 100% in spite of using the same symmetric bonding motifs of the earlier tetracene dimers.[9]

In this work, we report highly efficient intramolecular SEF in a new type of covalent dimer, with triplet yields of up to 192 ± 3%. The molecule used in this study, 13,13′-bis(mesityl)-6,6′-dipentacenyl (DP-Mes, **Figure 1**a), consists of two

S. Lukman, Dr. A. J. Musser, Dr. S. Athanasopoulos, Dr. C. K. Yong, Prof. R. H. Friend, Prof. N. C. Greenham
Cavendish Laboratory
University of Cambridge
Cambridge CB3 0HE, UK
E-mail: ncg11@cam.ac.uk

K. Chen, Dr. J. M. Hodgkiss
MacDiarmid Institute of Advanced Materials and Nanotechnology, and
School of Chemical and Physical Sciences
Victoria University of Wellington
Wellington 6010, New Zealand

Dr. Z. Zeng, Dr. Q. Ye, Dr. C. Chi, Prof. J. Wu
Department of Chemistry
National University of Singapore
3 Science Drive, 117543, Singapore
E-mail: chmwuj@nus.edu.sg



**DOI: 10.1002/adfm.201501537**

ADVANCED FUNCTIONAL MATERIALS
www.afm-journal.de



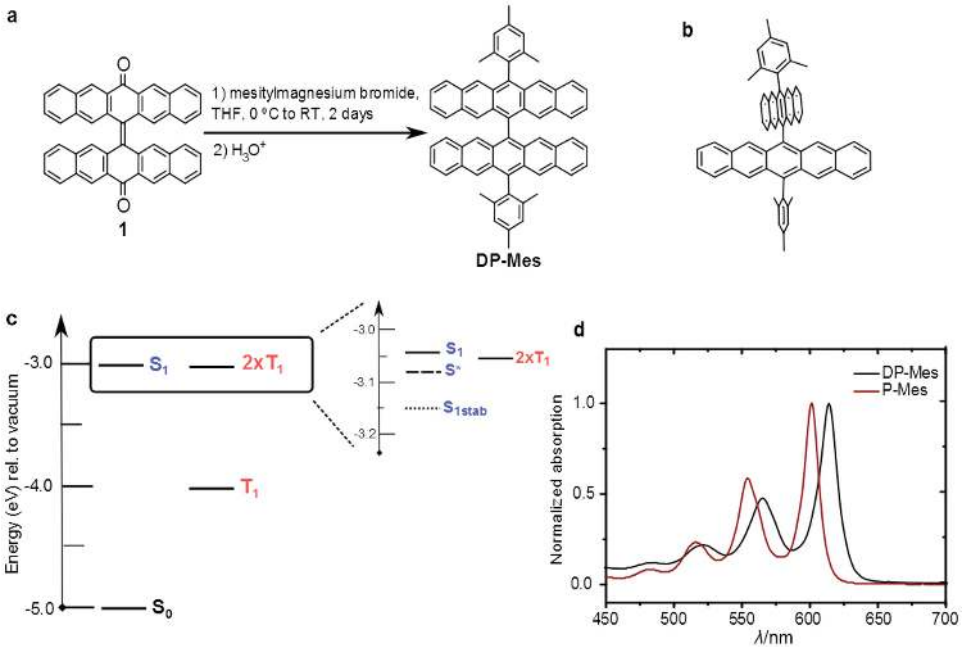


**Figure 1.** DP-Mes chemical and energetic structure. a) Chemical structure of precursor (1) and reaction conditions for DP-Mes formation. b) DFT-optimized (B3LYP/6–311G**) ground-state geometry of DP-Mes, demonstrating the orthogonality of the pentacenes (details in the Supporting Information). Hydrogen atoms omitted for clarity. c) Energy levels of DP-Mes measured in this work. $S_1$ is determined from absorption spectroscopy; S* and $S_{1stab}$ from long-lived photoluminescence in nonpolar and polar solvent, respectively; and $T_1$ from phosphorescence in polyethylene oxide matrix. d) Steady-state absorption spectra of DP-Mes and P-Mes in toluene. The DP-Mes spectrum exhibits no solvent dependence.

pentacenes directly bonded through a single C—C bond with two bulky mesityl groups at the *meso*-positions. The geometry of the dimer, with two nearly orthogonal pentacene cores, is unlike any structure currently proposed for efficient SEF and suggests there may be additional molecular design routes. Indeed, the intramolecular SEF process is robust, with sub-picosecond triplet formation in nonpolar and polar solvents and in dispersions within a range of polymer matrices. We observe slight variation in the rates of triplet formation but a significant change in the subsequent geminate annihilation across these systems. Our results highlight the importance of molecular geometry and coupling to charge-transfer configurations for SEF and triplet–triplet annihilation.

## 2. Results

### 2.1. Energetic Structure

We first consider the energy levels of DP-Mes and compare them to a single pentacene with the same solubilizing group (P-Mes). The HOMO and LUMO energies determined by cyclic voltammetry (Figure S8, Supporting Information) do not shift significantly with dimerization (**Table** 1). This is anticipated if the two pentacenes are nearly orthogonal to one another, and this geometry was confirmed in the solid state by X-ray crystallography (Figures S9 and S10, Supporting Information). Quantum chemical calculations using density functional theory indicate a similar conformation (88° between pentacenes, Figure 1b) in the gas phase. The same configuration was identified previously in a structurally related anthracene dimer (9,9′-bianthryl).[10–12] However, the absorption spectra reveal that dimerization has important photophysical effects in spite of this orthogonal structure. DP-Mes exhibits a clear vibronic progression similar to most soluble pentacene derivatives, but with a lower 0–1/0–0 peak ratio than P-Mes (0.5 vs 0.6, Figure 1d). The main absorption peaks are also slightly red-shifted (≈15 nm) from those of P-Mes, indicative of coupling between the chromophores. Indeed, the peak molar extinction coefficient of DP-Mes ($\varepsilon_{615}$ ≈ 7900 L mol$^{-1}$ cm$^{-1}$) is less than half that of P-Mes ($\varepsilon_{601}$ ≈ 17 000 L mol$^{-1}$ cm$^{-1}$). This value is only one quarter of what would be expected for a dimer of noninteracting pentacenes and is a strong demonstration of electronic coupling between the pentacenes. By contrast, the recent study of pentacene dimers separated by a phenyl spacer showed a doubling of extinction coefficient upon dimerization.[9] Likewise, earlier studies of 9,9′-bianthryl, diphenylisobenzofuran dimers and tetracene dimers all reveal weakly coupled chromophores with extinction coefficients twice those

**Table 1.** Electrochemical and optical properties of monomer (P-Mes) and dimer (DP-Mes). All values are reported in eV.

| Molecule | $E_{HOMO}$[a)] | $E_{LUMO}$[a)] | $E_{gap,electrochem}$ | $E_{gap,optical}$[b)] |
|---|---|---|---|---|
| P-Mes | −4.93 | −2.98 | 1.95 | 2.06 |
| DP-Mes | −5.06 | −2.98 | 2.08 | 2.02 |

[a)]Recorded $E_{1/2}$ values versus Ag/Ag$^+$ in $CH_2Cl_2$ with $TBAPF_6$ as supporting electrolyte. Energies of HOMO and LUMO electrochemical energy gaps calculated from the onset of the first oxidation and reduction waves in the cyclic voltammogram; [b)]Optical HOMO–LUMO gaps determined from the onset of lowest-energy visible steady-state absorption band. The onset is defined as the intersection between the baseline and a tangent line touching the point of inflection.




DOI: 10.1002/adfm.201501537

of the corresponding monomers.[7,13] These systems could be interpreted with singlet states initially localized on a single chromophore. DP-Mes is thus unique among covalent dimers based on singlet fission chromophores for showing strong hypochromism, and we conclude that even though the interaction between pentacene units in DP-Mes is small relative to pentacene films, they are not independent but should rather be treated as a single photophysical entity. On the basis of these findings, we consider the excited singlet state in DP-Mes to be delocalized over both halves of the dimer, as indicated by quantum chemical calculations (Figure S12, Supporting Information) and transient absorption spectra (see below).

### 2.2. Prompt and Delayed Photoluminescence

The photoluminescence (PL) spectra of DP-Mes at short (200 fs) and long (4 ns) delays after photoexcitation are shown in **Figure 2**a. Whereas monomeric pentacene derivatives tend to exhibit high PL quantum efficiency (>70%),[6] DP-Mes has an emission yield of only 4.2 ± 0.7% in toluene, rising to 8.3 ± 0.6% in *ortho*-dichlorobenzene (determined versus Rhodamine 101 in ethanol as reference).[11,14] We characterized the initial "prompt" PL decay in toluene solution using transient grating PL spectroscopy.[15] As can be seen in Figure 2b (filled circles, left), the emissive singlet state is rapidly depopulated, with an exponential lifetime of 750 fs in toluene ($\tau_{pr}$). The PL decay is still faster in *ortho*-dichlorobenzene (squares), with an initial time constant of 430 fs. Notably, in this more polar solvent the emission on the red edge of the spectrum (open squares) does not decay to zero but rather to some higher baseline, indicating the presence of a longer-lived red emitting species by 1 ps. We return to this phenomenon below. The rapid initial decay of photogenerated singlet excitons ($S_1$) in both solutions suggests a very efficient quenching channel.

Nevertheless, we also observe significant photoluminescence on longer time scales, which we define as "delayed" PL (Figure 2b, right). The delayed emission in toluene has a similar spectral profile to the prompt, with a slight redshift and broadening consistent with conformational relaxation to a nonorthogonal equilibrium geometry,[10] and decays with a lifetime of 2.3 ns ($\tau_{del}$, filled circles). The effect of solvent polarity in this regime is pronounced. In polar solvent we observe a further redshift of ≈20 nm and accompanying increase of the PL lifetime to 5.1 ns. This behavior is reminiscent of previous studies of 9,9′-bianthryl, which exhibits a significant redshift with loss of vibronic features in polar media due to the formation of a twisted intramolecular charge-transfer state.[10,16] However, the spectral shift and lifetime enhancement we observe are smaller than in 9,9′-bianthryl and, crucially, the long-lived PL exhibits a clear vibronic progression and decays uniformly across the entire spectrum in both solvents (Figure S15, Supporting Information). We find no evidence for the presence of more than one emissive species, such as a twisted intramolecular charge-transfer state, on the 100s of ps time scale and beyond. Instead, our results point to strong mixing with charge-transfer configurations in the singlet state. Consequently, while the initial singlet population (prompt PL) is the same in both solvents, dichlorobenzene enables much more substantial relaxation into the longer-lived emissive species. We consider these spectra to reflect a combination of solvent stabilization of the excited state and conformational relaxation into a nonorthogonal equilibrium geometry.[10,12,17] The latter effect is prevented in rigid polystyrene matrix, and indeed we can detect no long-lived emission in such films (see below). Given the rapid prompt PL decay, these measurements of delayed fluorescence require either that a sub-population of molecules is unable to undergo this initial decay or that a similar emissive species is regenerated on long time scales. Using transient absorption (TA) spectroscopy, we show below that both mechanisms can occur, depending on the molecular environment.

### 2.3. Intramolecular SEF

TA results in this paper are presented in units of ΔT/T, in which the absorption of photogenerated states appears negative and is termed photoinduced absorption (PIA). Positive features can reflect either an increase in transmission of the probe due to ground-state bleaching (GSB) or the detection of additional

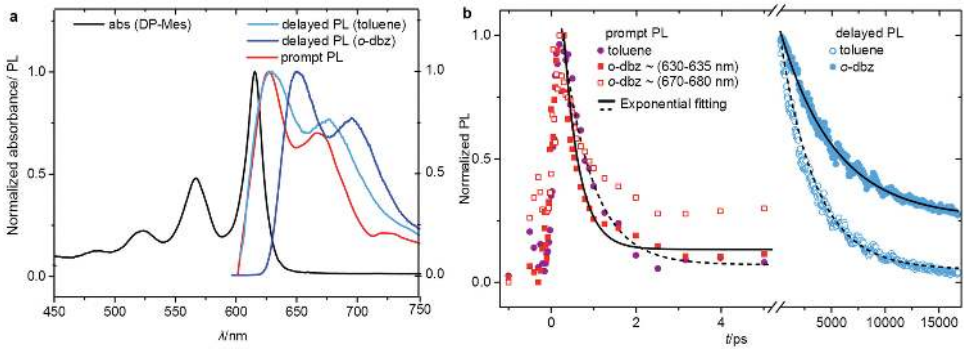


**Figure 2.** Prompt and delayed photoluminescence in solution. a) Normalized steady-state absorption spectrum of DP-Mes in toluene. Similar PL spectra at 200 fs (prompt PL) were measured in toluene and *ortho*-dichlorobenzene (*o*-dbz); only toluene data are shown for clarity. Spectra at 4 ns (delayed PL) were collected from toluene (light blue) and *o*-dbz (dark blue) solutions. b) Prompt PL kinetics for toluene and *o*-dbz solutions were averaged near the 0–0 peak (630–635 nm, filled symbols), and in *o*-dbz additionally at 670–680 nm. Delayed PL was measured at 660 nm. The relative scale of prompt and delayed PL is unknown, as they cannot be measured on the same system. Lines are monoexponential fits described in the text.

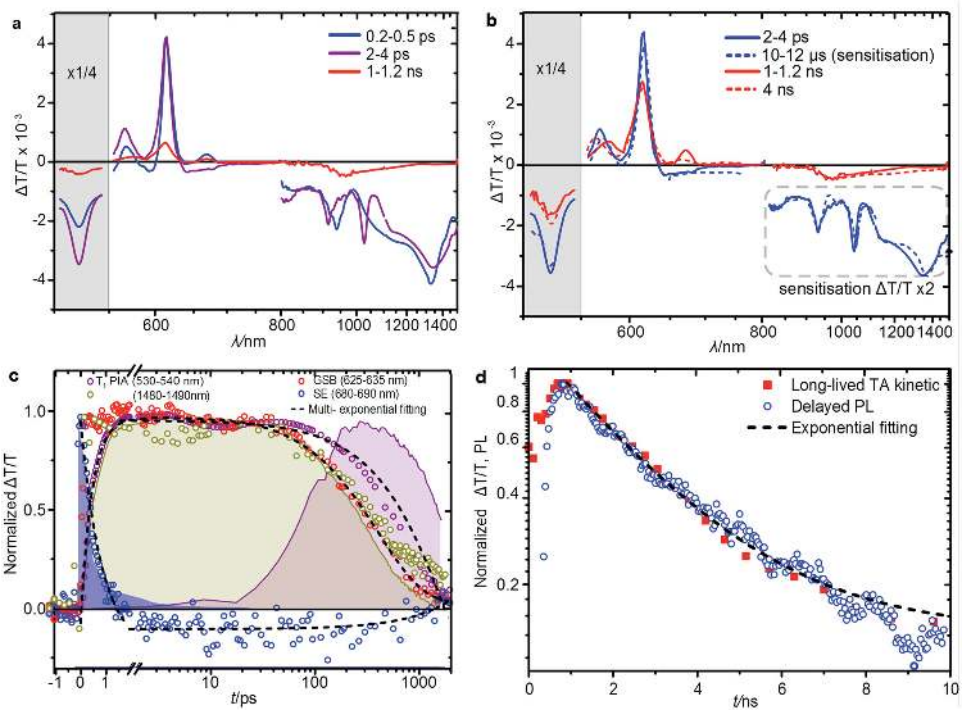


**Figure 3.** Transient absorption of DP-Mes in toluene. a) TA spectra of 10 mg $mL^{-1}$ solution, averaged over the indicated time ranges. The strong PIA < 550 nm is multiplied by a factor of 1/4 for clarity. b) Comparison of the TA spectrum at 2–4 ps with the long-lived triplet spectrum observed in sensitization (10–12 μs), and of the TA spectrum at 1–1.2 ns in Figure 3a (magnified) with the raw TA data at 4 ns. The sensitization spectrum in the NIR was scaled by a factor 2, as the triplet PIA is stronger relative to GSB following direct excitation. c) Kinetics of $T_1$ PIA (530–540 nm and 1480–1490 nm), GSB (625–635 nm), and SE (680–690 nm) from (a). The dashed lines are obtained from a global fit of the dataset with three exponential time constants (parameters in Table S7, Supporting Information). The coloured regions represent the normalized population kinetics of $S_1$ (blue), $T_1$ (yellow), and the long-lived species S* (purple) obtained from spectral decomposition. d) Normalized decay kinetics of the PIA at 1100 nm and the delayed PL of DP-Mes. The dashed line is a monoexponential fit with $\tau_3 = 2.3$ ns.

photons from stimulated emission (SE). Immediately following photoexcitation in toluene solution (**Figure 3**a and Figures S16–S18), we detect two strong positive peaks at 580 and 615 nm and a weak positive band that spans 660–700 nm. The first two peaks can be identified as GSB from their similarity to the ground-state absorption spectrum, while the weaker feature matches the prompt PL described above and can be assigned to SE. The SE decays with an exponential time constant of 760 fs (Figure 3c), matching the value determined from time-resolved fluorescence. In addition, two negative peaks are observed at 950 and 1300 nm along with a shoulder at 1075 nm. These decay with the same kinetics as the SE and can be identified as $S_1$ PIA.

As these singlet signatures decay, new spectral features appear, notably strong PIA bands peaked at 530 and 1380 nm; a distinctive trio of sharp bands at 810, 915, and 1045 nm; and a weak PIA at 650 nm (Figure 3a, 2–4 ps). These can all be identified as signatures of DP-Mes triplet excitons ($T_1$) from their similarity to the triplet PIA spectra observed in other acenes in solution.[6,18] We have confirmed this assignment using an established triplet sensitization experiment with a fullerene donor (Figure 3b, blue dashed; full spectra in Figure S19, Supporting Information).[19] Intriguingly, the shape of the sensitized triplet spectrum differs in one key respect: the PIA in the NIR is 50% weaker, relative to the GSB, than in the spectrum following direct excitation. In other words, direct excitation of DP-Mes yields twice as much triplet exciton PIA for the same quantity of excited dimer (GSB). The results in Figure 3 thus show complete depopulation of $S_1$ and conversion into $T_1$ within 2 ps following photoexcitation, a time scale too fast for intersystem crossing in the absence of heavy atoms. It follows that DP-Mes exhibits rapid intramolecular SEF, presumably resulting in one triplet exciton strongly localized on each pentacene unit,[20] and since we detect no competing decay channels it is likely to be highly efficient.

We highlight the behavior of the ground-state bleach (Figure 3c, red) during this process, with a focus on the band at 615–625 nm, where the singlet (0.2–0.5 ps) and triplet (2–4 ps) spectra align well and there appear to be no overlapping PIA or SE features (see Figure S20 of the Supporting Information for normalized comparison). The magnitude of this band, i.e. the population of dimers in an excited state, remains constant during triplet formation. We note that unlike solutions of TIPS-pentacene,[6] the two pentacene units in DP-Mes are permanently linked, and indeed must be more strongly coupled than in other pentacene dimers, as discussed above. We find that the singlet exciton is delocalized over the two pentacene units and it is not possible to locally photoexcite just one. At most one singlet exciton can be generated per molecule, and we observe similar decay kinetics



*Adv. Funct. Mater.* **2015**,
DOI: 10.1002/adfm.201501537

of $S_1$ irrespective of excitation density (Figure S18, Supporting Information), with no sign of intramolecular singlet–singlet annihilation within the accessible range. The important implication of these effects is that the singlet exciton removes the entire dimer from the ground state, in the same way as a pair of localized triplet excitons. The same conclusion arises from consideration of the triplet spectrum obtained via sensitization (one triplet), in which the relative magnitude of triplet PIA relative to GSB is half that following direct excitation (two triplets) (Figure S20, Supporting Information). These results require that the state described by the ground-state absorption and GSB is delocalized across the entire dimer, and consequently intramolecular SEF should increase the number of excitons present but leave the magnitude of GSB unchanged. The constant bleach during SEF thus indicates that the population of excited molecules does not significantly change and that there is no strongly competing decay back to the ground state. It demonstrates that fission proceeds with near-quantitative efficiency, as expected from the fast fission rate, a very surprising result for such an orthogonal, symmetric dimer. For ease of comparison across different experimental conditions, we follow the approach reported for TIPS-pentacene solutions to determine the triplet extinction coefficient (see the Experimental Section for details).[6] In toluene solution, the magnitude of $T_1$ PIA at 10 ps gives a triplet exciton yield of 192 ± 3%.

### 2.4. Geminate Triplet–Triplet Annihilation

Subsequent to SEF in toluene solution, the triplet population decays with a lifetime of 650 ps. This lifetime is significantly shorter than that of triplets produced via sensitization (13 µs, Figure S19, Supporting Information) and is completely independent of excitation power (Figure S18, Supporting Information). Such behavior suggests geminate intramolecular triplet–triplet annihilation (TTA) as the dominant decay pathway and constitutes further proof that the triplets must be generated in pairs. Once the signatures of $T_1$ have completely decayed, there remains a weak GSB signature indicating a small residual population and a broad new PIA centered at 1100 nm (Figure 3a,b, 1–1.2 and 4 ns time slices) revealing the presence of a distinct spectral species. We monitor this state on longer time scales using nanosecond excitation, and its decay closely matches the delayed PL kinetics discussed above (Figure 3d), identifying it as the final emissive state in nonpolar solution, which we label S*. The rise of this feature cannot be directly resolved due to overlap with the stronger $T_1$ PIA. Instead, we use a spectral decomposition procedure on the entire TA dataset presented in Figure 3. This approach utilizes a genetic algorithm to establish the individual spectra and population kinetics of the singlet, triplet, and the unidentified third species (see Supporting Information for details).[21] The advantage of this approach is that it does not presuppose any particular model connecting the states or any assignment as to their nature. The resulting population kinetics (Figure 3c, shaded regions) arise naturally and reproducibly from the data and illustrate a clear sequential relationship between $S_1$, $T_1$, and S*. This terminal species is formed at the expense of decaying $T_1$, and we accordingly assign it to a singlet state generated by triplet–triplet annihilation. We stress that this is a minority decay pathway: the strong reduction in GSB on these time scales indicates that TTA primarily returns the molecule to the ground state. The magnitude of GSB at 1.5 ns shows that roughly 10% of initially excited DP-Mes ends up in the S* state, which rules out that this and the accompanying PL signature are due to chemical defects or impurities in our analytically pure sample.

### 2.5. Triplet Generation and Annihilation under Geometric Constraint

We investigated the importance of geometric relaxation to the photophysics of DP-Mes by embedding the molecule in a series of polymer matrices with different glass transition temperatures: polystyrene (PS, $T_g \approx 95$ °C), polyvinyl acetate (PVAc, $T_g \approx 30$ °C) and polyethylene oxide (PEO, $T_g \approx <-30$ °C). At room temperature, this series affords a range of resistance against large-scale conformational relaxation in the singlet state.[10] While small conformational changes should still be possible, the two pentacene chromophores are expected to be held in the orthogonal ground-state configuration. In **Figure 4** we show the results of sub-ps TA measurements on these films. In all three matrices, we can identify the same initial spectral features described above for toluene solutions. Namely, singlet excitons are rapidly (sub-ps) converted into triplets while the ground-state bleach remains constant. The decay kinetics reveal that the rate of SEF is in fact enhanced in the presence of some degree of conformational restriction, with $\tau_{SEF} = 730$, 640, and 430 fs for PS, PVAc, and PEO matrices, respectively. This surprising result demonstrates that the orthogonal equilibrium geometry of the ground state is favorable for rapid and efficient SEF in spite of the poor $\pi$-orbital overlap. Furthermore, we see that fission proceeds faster in the more polar environments of PVAc and especially PEO, a sign of the role of charge-transfer configurations in the underlying mechanism. Though charge-transfer states are never directly populated, we propose that the polar environment stabilizes these configurations, resulting in enhanced coupling to both the singlet and triplet-pair states.[22] We investigate this possibility in more detail below in polar solvent. Assuming the ratio of singlet to triplet absorption cross-section is the same in these matrices as in toluene, we can extract triplet yields with the same procedure: 191 ± 4%, in PS, 187 ± 3% in PVAc and 188 ± 5% in PEO.

The subsequent process of TTA, however, is strongly affected. The triplet lifetime in the most rigid PS films increases to 1.1 ns, and we detect no signature of the final emissive state seen in nonpolar solution. The PL quantum efficiency of DP-Mes in this matrix is correspondingly reduced to 0.8 ± 0.1%, which we consider to reflect the emission intensity from the prompt pathway. The slight reduction of the film rigidity in PVAc returns the same behavior seen in toluene: TTA results in the generation of S*, on a time scale of 1.2 ns. We thus conclude that the ability to form S* is closely linked to conformational relaxation in the triplet excited state. Interestingly, upon further reduction of $T_g$ in the softest matrix, PEO, we observe a dramatic enhancement of the triplet lifetime to 143 ns. The fast geminate TTA channel is completely suppressed, enabling

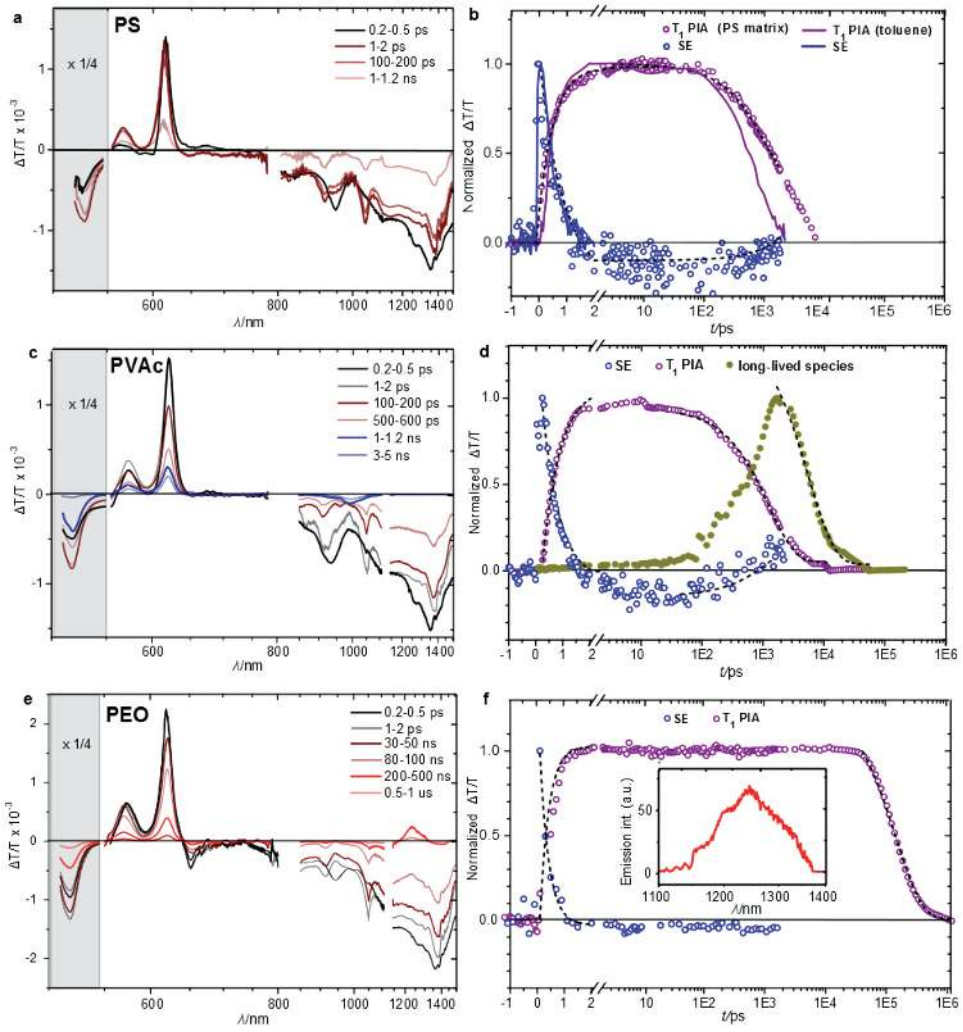


**Figure 4.** Transient absorption of DP-Mes in polymer matrices. a,c,e) TA spectra, averaged over the indicated time ranges, for DP-Mes embedded in rigid PS, intermediate PVAc or viscous PEO matrices. The strong PIA < 550 nm is multiplied by a factor of 1/4 for clarity. b,d,f) Normalized kinetics of $T_1$ PIA (530–540 nm) and SE (670–680 nm) in polymer matrices. Dashed lines are obtained from global fits of the datasets with two (PS and PEO) or three (PVAc) exponential time constants. All fitting parameters are in Table S8, Supporting Information. In (b), PS matrix data (circles) are compared to equivalent kinetics in toluene solution (solid line). In (d), population kinetics of the S*-like species (filled circles) are extracted from the same spectral decomposition used for toluene solution, due to the overlap of spectral features. Inset in (f) shows phosphorescence collected under CW illumination.

detection of phosphorescence (inset, Figure 4f) and a direct determination of the triplet exciton energy of 1 eV. This value is unexpectedly high and reveals a significant perturbation of the pentacene energetic landscape upon dimerization, resulting in a strong reduction of the driving force for SEF relative to pentacene and its derivatives.[20]

### 2.6. Solvent Polarity Dependence of SEF

A similar series of measurements was performed on solutions of DP-Mes in *ortho*-dichlorobenzene to investigate the influence of solvent polarity and possible role of charge-transfer states. In this system, we no longer observe formation of a longer-lived emissive state via TTA and instead find that a substantial fraction of the initial singlet population is unable to undergo SEF. As shown in **Figure 5**, we again observe rapid intramolecular SEF, but the reduced prominence of the triplet peaks relative to the singlet PIA indicates the efficiency is lower than in toluene. From the magnitude of $T_1$ PIA at 10 ps, we extract a triplet yield of 150%. The lower yield is surprising, as analysis of the decay kinetics in Figure 5b shows that the rate of SEF in this solution is significantly faster ($\tau_{SEF} \approx 390$ fs, vs 750 fs in toluene), which points to the importance of coupling to charge-transfer configurations to drive singlet fission, even when the charge-transfer state is not directly populated.[22,23] Performing the same spectral decomposition used above for toluene solutions, we confirm that ≈15% of the initial singlet population survives the rapid SEF regime (Figure 5b, blue-shaded plateau region). The signature of this population can be clearly observed in the PIA peaks in the NIR that form immediately upon excitation and are still present at 1–1.2 ns.




DOI: 10.1002/adfm.201501537

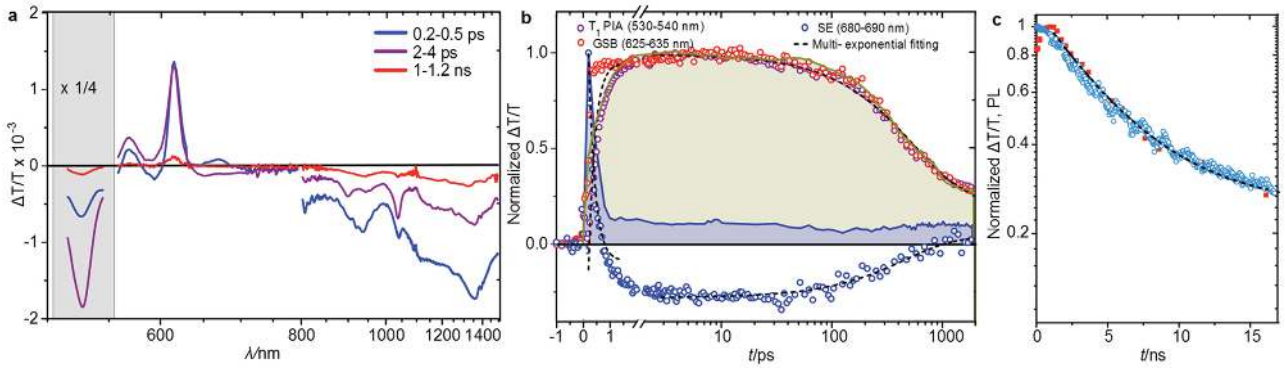


**Figure 5.** Transient absorption of DP-Mes in *o*-dbz. a) TA spectra of 10 mg mL$^{-1}$ solution, averaged over the indicated time ranges. The strong PIA <550 nm is multiplied by a factor of 1/4 for clarity. b) Kinetics of $T_1$ PIA (530–540 nm), GSB (625–635 nm), and SE (680–690 nm) from (a). The dashed lines are obtained from a global fit of the dataset with three exponential time constants (in Table S9, Supporting Information). The coloured background represents the normalized population kinetics of $S_1$ (blue) and $T_1$ (yellow) obtained from spectral decomposition. c) Normalized decay kinetics of the PIA at 940 nm and the delayed PL of DP-Mes in *o*-dbz. The dashed line is a monoexponential fit with $\tau_3 = 5.1$ ns.

These excitons are found to decay on the same 5 ns time scale (Figure 5c) as the significantly red-shifted delayed PL described above, allowing us to assign these signatures to a stabilized singlet $S_{1stab}$ and confirming, as in toluene, that they do not arise from trace impurities. This residual singlet population is responsible for the increase of PL quantum yield to 8%. We recall that this red-emitting species survives the rapid initial PL decay in Figure 2b, suggesting a branched decay pathway in polar solvent into two separate channels. Using the yields and time constants above, simple rate analysis suggests that in this polar solution SEF ($k_{SEF} \approx 2.1$ ps$^{-1}$) is in direct competition with singlet stabilization ($k_{stab} \approx 0.4$–$0.7$ ps$^{-1}$) below the energetic threshold for triplet formation (≈2 eV). The intrinsic time constant of the latter process, 1.4–2.3 ps, is consistent with solvent rearrangement to stabilize the singlet state.[24] As seen previously, the triplet pairs that do form decay much faster than individual triplets generated through sensitization. We assign the triplet lifetime of 830 ps to geminate TTA. No additional electronic state beyond $S_1$ and $T_1$ can be detected on these time scales, meaning TTA efficiently returns the system to the ground state.

## 3. Discussion

It is instructive to compare the behavior we observe to the closely related anthracene dimer, 9,9′-bianthryl. This molecule exhibits many of the same properties as DP-Mes: an orthogonal ground-state geometry, a nonorthogonal singlet equilibrium geometry and solvent-dependent photoluminescence. Immediately following photoexcitation, 9,9′-bianthryl undergoes rapid, unhindered conformational relaxation on sub-picosecond time scales.[12] Our observation of singlet fission in DP-Mes with comparable rates suggests that nuclear relaxation and triplet-pair formation may be coupled, as they are in TIPS-pentacene films.[25] An important distinction between the molecules is the later evolution in polar media. The anthracene dimer is well known for forming a twisted intramolecular charge-transfer state in the picosecond regime.[26] In DP-Mes, we detect no spectral evolution on such time scales, and indeed we find no spectral features that match the DP-Mes radical cation or anion profiles (see Figure S22, Supporting Information). The even faster process of singlet fission may preclude formation of that state. Nonetheless, the polarity dependence of the triplet formation rate and yield demonstrates that these charge-transfer configurations continue to play an indirect role, possibly also coupled to conformational relaxation. One of the established models of SEF proposes that triplet formation is mediated by indirect coupling to charge-transfer states.[22] From analogy to 9,9′-bianthryl, we speculate that the charge-transfer state has the same symmetry and orthogonal equilibrium geometry as the ground state.[11] Our results in rigid polymer matrices indicate that this orthogonal geometry is favorable for singlet fission, which can be related to effective coupling via the charge-transfer state in that conformation. As geometric relaxation proceeds and the charge-transfer character decreases, this indirect coupling would weaken and may eventually halt SEF, as seen in polar solution. The PEO matrix offers a similar enhancement to the fission rate, but restriction of conformational relaxation and the lack of solvent reorganization prevent the competing decay channel into $S_{1stab}$ and the triplet yield remains high.

The other process evaluated in this work, geminate triplet–triplet annihilation, is less well understood. The triplet decay observed in the rigid matrix and polar solvent is markedly faster than the typical bimolecular TTA time scales measured in acenes in the solid state.[27] On the other hand, it is much slower than the geminate TTA observed in polyenes such as poly(3-dodecylthienylenevinylene),[19] where the presence of a low-lying excited state of the same symmetry allows rapid coupling to the ground state. We see no direct evidence for low-lying excited states in DP-Mes that would facilitate TTA, but detailed theoretical studies are called for to investigate the possibility more fully. In the absence of such a state, the majority of triplets likely annihilate through multiphonon emission, as has been proposed in crystalline pentacene.[27] It is possible that the fast recombination we observe can also be attributed in part to the enforced proximity of the two triplets, with a consequently high annihilation attempt frequency. The difference in triplet lifetime between PS film, *ortho*-dichlorobenzene solution and PEO film, presumably related to molecular conformation or charge-transfer states, indicates that this is not the only

explanation. It is likely to be an important factor, though, and we propose that the lack of fast geminate TTA in most acene films requires the triplets generated by SEF to quickly separate by more than the DP-Mes interchromophore distance of ≈4.5 Å.

The special case of TTA in toluene and PVAc matrix raises further questions. While the majority of triplets annihilate through the same pathway as in the other systems, a new emissive singlet state is also populated in sufficient yield to be detected in TA. Singlet regeneration from TTA has been extensively characterized in tetracene,[28] where SEF is slightly endothermic and thus the reverse process TTA is exothermic and favorable. It has never been observed in pentacene-based systems, which exhibit exothermic SEF.[4] DP-Mes is unique in this regard: dimerization significantly perturbs the triplet energetic structure, even though the $S_0 \rightarrow S_1$ transition remains similar. The resulting reduction of TTA endothermicity can explain the appearance of this weak emissive decay channel. The kinetics observed in toluene and PVAc matrix indicate an unusual energetic relationship between $S_1$, the pair of triplets and S*. The initial process of SEF must be energetically favorable to proceed so quickly, and similarly the emissive state formed through TTA would be expected to re-form triplet pairs. There is no evidence, however, of any further SEF within the lifetime of S*, hence it must be sufficiently distinct from $S_1$ that photoluminescence becomes the more efficient decay pathway. Comparison with the results from PS matrix and polar solution leads us to propose that the product of "emissive TTA" is a geometrically relaxed singlet state. Such geometric relaxation may alter the coupling of the singlet to charge-transfer configurations,[11] and consequently the ability of the state to undergo SEF.[4]

## 4. Conclusions

Our results reveal that fast and efficient SEF can occur within a molecular dimer in a range of conditions and highlight the importance of interchromophore geometry and solvation dynamics. We see the most efficient triplet formation in toluene, where PL spectroscopy shows only slight geometric relaxation within the emissive states. Likewise, DP-Mes dispersed in polymer matrices is firmly held in the orthogonal geometry of the ground state, and there appear to be no alternative processes to intramolecular SEF. The introduction of polar solvent alters the excited-state energetic landscape, allowing relaxation into stabilized $S_{1stab}$ to directly compete with SEF. We then observe faster triplet formation, but with lower overall yield. When the molecule is conformationally restricted, the same polarity-induced enhancement of fission rate is observed, but with parasitic $S_{1stab}$ formation suppressed. This behavior points to a subtle interplay of the energies of $S_1$, the triplet pair state, $S_{1stab}$ and charge-transfer states, as well as the strength of the couplings between them. These properties, in turn, closely depend on molecular geometry and suggest a role for nuclear relaxation in controlling SEF and TTA.

## 5. Experimental Section

*Dimer Synthesis*: The precursor for DP-Mes was 6,6′-bispentacenequinone **1** (Figure 1a), which was prepared using established procedures.[29] A solution of mesityl magnesium bromide solution in ether (1 M, 1.7 mL) was added to a solution of compound **1** (100 mg, 0.171 mmol) in THF (30 mL) at 0 °C under argon atmosphere. The reaction mixture was allowed to warm to room temperature and stirred for 48 h. After quenching with HCl (1 M, 2 mL), the mixture was diluted with ether (60 mL) and washed with water (10 mL). After solvent evaporation, the crude product was purified with column chromatography on silica gel (DCM:hexane, 1:15 v/v) to give target compound DP-Mes as a deep blue solid (99 mg, 73% yield). Interestingly, no reducing agent such as $SnCl_2$ is required for reduction of the diol intermediate. Details of P-Mes (single-pentacene equivalent to DP-Mes) synthesis, NMR characterization, and X-ray crystallographic characterization of P-Mes and DP-Mes can be found in the Supporting Information. Samples used for spectroscopy were analytically pure by NMR and high resolution mass spectrometer analysis.

*Sample Preparation*: The mesityl side groups on DP-Mes provide chemical stability and render significant solubility. We have utilized this property to study well isolated molecules of DP-Mes in solution or dispersed in polymer matrices. Unless otherwise noted, all measurements in this work were performed on solutions at 10 mg $mL^{-1}$ in either toluene or *ortho*-dichlorobenzene, prepared and sealed under nitrogen atmosphere. The same photophysical behavior was observed at 1.0 and 0.1 mg $mL^{-1}$ (Figure S17, Supporting Information), confirming that our results only describe intramolecular processes. Triplet sensitization was performed using established procedures,[19] with a mixed toluene solution of 1 mg $mL^{-1}$ DP-Mes and 3 mg $mL^{-1}$ *N*-methylfulleropyrrolidine. All solution measurements were performed in 1 mm light-path quartz cuvettes (Hellma Analytics). To prepare films with dispersed DP-Mes, stock solutions of 10 mg $mL^{-1}$ DP-Mes and 100 mg $mL^{-1}$ polystyrene, polyethylene oxide or polyvinyl acetate in toluene were mixed together to obtain a final DP-Mes concentration of 1 mg $mL^{-1}$ with a DP-Mes:polymer weight ratio of 1:100. This mixture was cast on Spectrosil quartz substrates and spun at 800 rpm for 60 s in nitrogen atmosphere.

*Photoluminescence Spectroscopy*: The PL of DP-Mes was measured in two distinct temporal regimes. Fast (sub-100 ps) photoluminescence dynamics were studied using the transient grating technique described in detail by Chen et al.[15] Longer-time dynamics were recorded with a standard time-correlated single-photon counting system (Edinburgh Instruments), using 40 MHz excitation at 470 nm (PicoQuant), and delayed photoluminescence spectra were collected with an intensified CCD (iStar DH740, Andor Instruments) following excitation with a narrow-band NOPA centered at ≈530 nm. Phosphorescence was detected using a calibrated infrared InGaAs photodiode array (ANDOR iDus 490A) coupled to a spectrograph (ANDOR Shamrock), with CW excitation at 532 nm (0.7 mW).

*Transient Absorption Spectroscopy*: Transient absorption measurements were performed on a previously reported setup.[19,30] Briefly, broadband probe pulses were generated using noncollinear optical parametric amplifiers (NOPAs) built in-house to cover three separate spectral ranges: 500–800, 800–1100, and 1100–1500 nm.[31] The same InGaAs array detector (Hamamatsu G11608–512) was used for all wavelengths. For sub-picosecond measurements, the samples were pumped with the 620 nm output from an automated OPA (TOPAS, Light Conversion), with a pulse duration of <200 fs. The sub-ps setup is limited by the length of the mechanical delay stage to delays of 2 ns. Further spectral evolution of DP-Mes and triplet sensitization were investigated using excitation with the ≈1 ns output of a frequency-doubled (532 nm) Q-switched Nd-$YVO_4$ laser (Advanced Optical Technologies), which was externally triggered with an electronic pulse. For these measurements, strong pump scatter in the spectral range 520–540 nm required removal of this probe region. In all measurements, pump and probe polarizations were set to magic angle (54.7°). Typical excitation densities were $10^{14}$–$10^{15}$ photons $pulse^{-1}$ $cm^{-2}$, and all decay kinetics were found to be independent of pump intensity (Figure S18, Supporting Information).




DOI: 10.1002/adfm.201501537

*Triplet Yield Determination*: The yield of triplet excitons in DP-Mes was determined by following the method of Walker et al.[6] Briefly, the ratio of singlet and triplet oscillator strengths were determined at a given wavelength through normalization of the spectra at the GSB. The approach here is based on the following assumptions: (1) the initial singlet exciton is delocalized over the entire DP-Mes molecule and thus bleaches both pentacene cores, as described in the main text; (2) a single triplet exciton on DP-Mes also bleaches the entire molecule; (3) the overlap of the TA spectral shape of $S_1$ and $T_1$ in the range 615–625 nm is due to the absence of overlapping features (SE and PIA) in this region, allowing the $T_1$ spectrum to be normalized relative to $S_1$; and (4) the PIA of two triplet excitons on DP-Mes is twice that of a single triplet. Assumption 2 follows directly from the optical evidence of interchromophore coupling (such as a 75% reduction in extinction coefficient per pentacene). Covalent bonding to a second pentacene strongly alters the absorption of the first, and it is reasonable to expect that anything that affects the absorption of one of these pentacenes (such as a localized triplet exciton) should accordingly alter the absorption of the entire molecule. Any such alteration of the absorption spectrum is precisely what is measured by GSB, which is insensitive to the nature of the excitations present. As for the third assumption, it is noted that the constant GSB is observed in that region during SEF requires either that there are no overlapping features or that they precisely and coincidentally balance out, which is considered highly unlikely. Thus, the triplet sensitization spectrum is treated as having the same underlying GSB (i.e., of the entire molecule) as the singlet spectrum, and can normalize $T_1$ relative to $S_1$ to determine the triplet oscillator strength. The final assumption is a consequence of the nature of PIA, which should be sensitive to the nature and directly proportional to the number of excitons present in the system. From the change in decay kinetics between triplets generated through sensitization and direct excitation, it is evident that DP-Mes is capable of supporting two localized triplet excitons, and it stands to reason that each can be excited into higher-lying triplet states.

Given these assumptions, two parameters were needed to calculate the triplet yield: the ratio the excited-state molar extinction coefficients ($\varepsilon^*$) for singlet and triplet states, and the ratio of the singlet and triplet excited state absorption under direct excitation. To determine the ratio of $\varepsilon^*$, the PIA of $S_1$ at 300 fs (the peak of our instrument response, when the stimulated emission is maximum) and the PIA of $T_1$ obtained from sensitization were compared, scaled such that the GSB of each has the same magnitude over 615–625 nm (see Figure S20 of the Supporting Information for normalized spectra). We then apply the formula below, using PIA magnitudes taken at 300 fs (initial $S_1$ population) and 10 ps ($T_1$ population following SEF) after direct excitation

$$\text{Triplet yield} = \frac{\Delta A(T_1)|_{t=10\,\text{ps}}}{\Delta A(S_1)|_{t=300\,\text{fs}}} \times \frac{\varepsilon^*_{S1}}{\varepsilon^*_{T1}} \quad (1)$$

In the case of *o*-dbz solution, the contribution of the residual $S_{1stab}$ population was first removed from the signal at 10 ps via spectral decomposition. Details of the calculations at particular probe wavelengths are presented in the Supporting Information.

[CCDC contains the supplementary crystallographic data for this paper. These data can be obtained free of charge from The Cambridge Crystallographic Data Centre via www.ccdc.cam.ac.uk/data_request/cif. The data underlying this paper are available at https://www.repository.cam.ac.uk/handle/1810/248998.]

## Supporting Information

Supporting Information is available from the Wiley Online Library or from the author.

## Acknowledgements

The authors thank Dr. Simon Gelinas and Dr. Akshay Rao for helpful discussions. J.W. acknowledges financial support from Singapore MOE Tier 3 grant (MOE2014-T3–1–004). S.L. thanks AGS Scholarship support from the A*STAR Singapore. The work was supported by the EPSRC (Grant No. EP/G060738/1). The authors acknowledge the use of the Darwin Supercomputer of the University of Cambridge High Performance Computing Service (http://www.hpc.cam.ac.uk/) and the EPSRC UK National Service for Computational Chemistry Software (NSCCS) at Imperial College London in carrying out this work.

Received: April 16, 2015
Revised: June 15, 2015
Published online:

[1] W. Shockley, H. J. Queisser, *J. App. Phys.* **1961**, *32*, 510.
[2] M. B. Smith, J. Michl, *Annu. Rev. Phys. Chem.* **2013**, *64*, 361.
[3] a) B. Ehrler, M. W. B. Wilson, A. Rao, R. H. Friend, N. C. Greenham, *Nano Lett.* **2012**, *12*, 1053; b) D. N. Congreve, J. Lee, N. J. Thompson, E. Hontz, S. R. Yost, P. D. Reusswig, M. E. Bahlke, S. Reineke, T. Van Voorhis, M. A. Baldo, *Science* **2013**, *340*, 334.
[4] S. R. Yost, J. Lee, M. W. Wilson, T. Wu, D. P. McMahon, R. R. Parkhurst, N. J. Thompson, D. N. Congreve, A. Rao, K. Johnson, *Nat. Chem.* **2014**, *6*, 492.
[5] M. W. B. Wilson, A. Rao, B. Ehrler, R. H. Friend, *Acc. Chem. Res.* **2013**, *46*, 1330.
[6] B. J. Walker, A. J. Musser, D. Beljonne, R. H. Friend, *Nat. Chem.* **2013**, *5*, 1019.
[7] a) A. M. Muller, Y. S. Avlasevich, W. W. Schoeller, K. Mullen, C. J. Bardeen, *J. Am. Chem. Soc.* **2007**, *129*, 14240; b) J. C. Johnson, A. Akdag, M. Zamadar, X. Chen, A. F. Schwerin, I. Paci, M. B. Smith, Z. k. Havlas, J. R. Miller, M. A. Ratner, *J. Phys. Chem. B* **2013**, *117*, 4680.
[8] P. J. Vallett, J. L. Snyder, N. H. Damrauer, *J. Phys. Chem. A* **2013**, *117*, 10824.
[9] J. Zirzlmeier, D. Lehnherr, P. B. Coto, E. T. Chernick, R. Casillas, B. S. Basel, M. Thoss, R. R. Tykwinski, D. M. Guldi, *Proc. Natl. Acad. Sci. USA* **2015**.
[10] K. Elich, M. Kitazawa, T. Okada, R. Wortmann, . *J. Phys. Chem. A* **1997**, *101*, 2010.
[11] G. Grabner, K. Rechthaler, G. Köhler, *J. Phys. Chem. A* **1998**, *102*, 689.
[12] M. Jurczok, P. Plaza, M. M. Martin, Y. H. Meyer, W. Rettig, *Chem. Phys.* **2000**, *253*, 339.
[13] a) H. D. Becker, V. Langer, J. Sieler, H. C. Becker, *J. Org. Chem.* **1992**, *57*, 1883; b) B. Valeur, M. N. Berberan-Santos, *Molecular Fluorescence: Principles and Applications*, John Wiley & Sons, Weinheim, Germany **2012**.
[14] T. Karstens, K. Kobs, *J. Phys. Chem.* **1980**, *84*, 1871.
[15] K. Chen, J. K. Gallaher, A. J. Barker, J. M. Hodgkiss, *J. Phys. Chem. Lett.* **2014**, *5*, 1732.
[16] Z. R. Grabowski, K. Rotkiewicz, W. Rettig, *Chem. Rev.* **2003**, *103*, 3899.
[17] G. D. Scholes, T. Fournier, A. W. Parker, D. Phillips, *J. Chem. Phys.* **1999**, *111*, 5999.
[18] Y. Meyer, R. Astier, J. Leclercq, *J. Chem. Phys.* **1972**, *56*, 801.
[19] A. J. Musser, M. Al-Hashimi, M. Maiuri, D. Brida, M. Heeney, G. Cerullo, R. H. Friend, *J. Am. Chem. Soc.* **2013**, *135*, 12747.
[20] S. L. Bayliss, A. D. Chepelianskii, A. Sepe, B. J. Walker, B. Ehrler, M. J. Bruzek, J. E. Anthony, N. C. Greenham, *Phys. Rev. Lett.* **2014**, *112*, 238701.
[21] S. Gélinas, O. Paré-Labrosse, C.-N. Brosseau, S. Albert-Seifried, C. R. McNeill, K. R. Kirov, I. A. Howard, R. Leonelli, R. H. Friend, C. Silva, *J. Phys. Chem. C* **2011**, *115*, 7114.

[22] T. C. Berkelbach, M. S. Hybertsen, D. R. Reichman, *J. Chem. Phys.* **2013**, *138*, 114103.
[23] D. Beljonne, H. Yamagata, J. Brédas, F. Spano, Y. Olivier, *Phys. Rev. Lett.* **2013**, *110*, 226402.
[24] a) J. R. Lakowicz, *Principles of Fluorescence Spectroscopy*, Springer Science & Business Media, New York, NY, USA **2013**; b) V. Sharma, N. Thakur, *Z. Naturforsch., A: Phys. Sci.* **2008**, *63*, 93; c) V. P. Pawar, *J. Chem. Eng. Data* **2006**, *51*, 882.
[25] A. J. Musser, M. Liebel, C. Schnedermann, T. Wende, T. B. Kehoe, A. Rao, P. Kukura, *Nat. Phys.* **2015**, *11*, 352.
[26] N. Mataga, H. Yao, T. Okada, W. Rettig, *J. Phys. Chem.* **1989**, *93*, 3383.
[27] A. D. Poletayev, J. Clark, M. W. Wilson, A. Rao, Y. Makino, S. Hotta, R. H. Friend, *Adv. Mater.* **2014**, *26*, 919.
[28] C. J. Bardeen, *Annu. Rev. Phys. Chem.* **2014**, *65*, 127.
[29] a) E. Clar, *Chem. Ber.* **1949**, *82*, 495; b) X. Zhang, X. Jiang, J. Luo, C. Chi, H. Chen, J. Wu, *Chem. Eur. J.* **2010**, *16*, 464.
[30] A. Rao, M. W. Wilson, J. M. Hodgkiss, S. Albert-Seifried, H. Bässler, R. H. Friend, *J. Am. Chem. Soc.* **2010**, *132*, 12698.
[31] D. Brida, C. Manzoni, G. Cirmi, M. Marangoni, S. Bonora, P. Villoresi, S. D. Silvestri, G. Cerullo, *J. Opt.* **2010**, *12*, 013001.




DOI: 10.1002/adfm.201501537